Measurement of the bending vibration frequencies of a rotating turbo wheel using an optical fibre reflective sensor

J Slavič[1]**, P Čermelj**[1]**, A Babnik**[1]**, J Rejec**[2]**, J Možina**[1] **and M Boltežar**[1]

[1] University of Ljubljana, Faculty of Mechanical Engineering, Aškerčeva 6, 1000 Ljubljana, Slovenia
[2] Domel d.d., 4228 Železniki, Slovenia

E-mail: Miha.Boltezar@fs.uni-lj.si

Abstract
An optical fibre reflective sensor was used to analyse the vibrations of a rotating turbo wheel up to 20 400 rpm. The measured signal required correction because of the natural unevenness of the turbo wheel and because of the variable deflection. Because the turbo wheel was rotating the signal became distorted and so we used a special method to extract the frequencies of the vibrations from the power spectra. The analysis showed increased intensity of the first three natural frequencies with an increased speed of rotation. The experimental results match very well with those obtained by numerical computation.

Keywords: rotating turbo wheel, disc, natural frequency, frequency extraction, optical fibre, distortion

1. Introduction

For the sake of reliable and quiet structures we need to know their vibration properties. To check the analytical and numerical approach, additional tests are often made on already-manufactured structures.
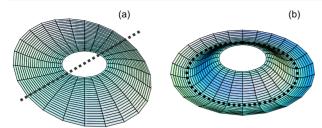
This paper is focused on the measurement and interpretation of the bending vibrations of a rotating turbo wheel. A disc can be a good approximation for more complex structures such as computer disks, circular saws, the turbo wheel of a suction unit etc. For the measurement of vibrations there are two major approaches: the contact approach and the non-contact approach.

Using a strain gauge is a contact approach; it can be used when the influence of the mass of the strain gauge and the other necessary equipment is negligible. However, in this case problems can occur with the transmission of the signal from the rotating object to the stationary surroundings.

Some non-contact approaches include measurement with an inductance-type displacement transducer [1–3] and measurement with a laser sensor. In the case of laser sensors, researchers usually use laser interferometry [4, 5], but alternatively, an optical fibre reflective (OFR) sensor can be used—as in the case of our experiment. Blade-tip-timing measurements are often used for measuring the vibration of rotor blades [6–8]. While in blade-tip-timing measurements the OFR sensor is used as a switch sensor, we used it as a displacement sensor. In spite of the fact that the principle of the OFR sensor has been known for years [9,10], we did not find any similar approaches to the measurement of the vibration of a rotating disc.

In order to study the axial vibration pattern on a rotating disc two different approaches can be used: the Eulerian or the Lagrangian [4]. In the first case the laser spot measures different points at different times; however, because the disc rotates there are problems with the 'speckle effect' [11] and the signal also becomes distorted. In the second case (the Lagrangian) we use mirrors to point the laser spot at the same measurement point every time [4, 5], so the problem of the signal distortion and the influence of the surface roughness is less noticeable. However, the second approach is less

Figure 1. Vibration mode with one diametrical node ($n = 1$) (*a*) and vibration mode with one circular node ($m = 1$) (*b*).
(This figure is in colour only in the electronic version)

appropriate for the case of high-speed rotation, because the mirrors cannot manage to track the measurement point.

The above-mentioned researchers used either the acoustic or electro-magnetic excitation of vibrations. In our case we used the excitation of the gyroscopic effect.

In the first section of this paper we present a review. In the next section we provide the background necessary for an interpretation of the measured signal. The third and fourth sections present experimental and numerical results, respectively. The fifth section compares these two approaches.

2. Theoretical background

Although rotating-disc vibration is represented by an infinite number of vibration modes, it is usually dominated by the response of a limited number of modes. A mode is uniquely represented by the number of nodal circles ($m = 0, 1, \ldots$) and the number of nodal diameters ($n = 1, 2, \ldots$) (figure 1). In the case when the axial displacement of a rotating plane is measured from a stationary point in the surroundings (figure 2), a distortion of the vibration signal appears.

The background to the interpretation of this distortion is shown in the following section.

2.1. A geometric model of disc vibration

This model describes the vibration of a rotating disc in the axial direction, as seen at a constant distance from the axis of rotation (figure 2). The model assumes that the specific modes can be superpositioned.

2.1.1. Vibration with diametrical nodes. A description of vibration can be very complex, but for the sake of simplicity the displacement (at a given distance from the axis of rotation) can be approximated by

$$N_n(\varphi, t) = \underbrace{\sin n\varphi}_{n\text{th mode}} \overbrace{\sin 2\pi \nu_n t}^{\text{vibration with time}} \qquad (1)$$

where ν_n is the natural frequency of vibration with n diametrical nodes and $\varphi \in (0, 2\pi)$ is the angle. The assumption of a maximum amplitude of unit size is made.

2.1.2. Vibration with circular nodes. If, at a given distance from the axis of rotation, the amplitude is constant (assumed to be equal to unity), then the vibration depends only on time:

$$M_m(t) = \sin 2\pi \nu_m t \qquad (2)$$

where ν_m is the mth natural frequency of vibration with m circular nodes.

2.1.3. The influence of the surface. The OFR sensor measures the local surface displacement as well as the surface unevenness and roughness. This impact can be approximated by a periodical, but not necessarily smooth, function:

$$X(\varphi) = X(\varphi + 2\pi a) \qquad a \in \mathbb{N}. \qquad (3)$$

2.1.4. Superposition of derived influences. At a given angle, time, and distance from the axis of rotation the approximation of the measured signal is (equations (1)–(3))

$$f(\varphi, t) = \sum_n N_n(\varphi, t) + \sum_m M_m(t) + X(\varphi). \qquad (4)$$

If the disc is rotating at a constant angular velocity (5) of frequency ν then equation (4) depends only on time (6).

$$\varphi(t) = 2\pi \nu t \qquad (5)$$

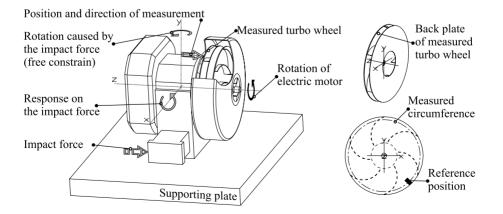$$f(t) = \sum_n N_n(\varphi(t), t) + \sum_m M_m(t) + X(\varphi(t)). \qquad (6)$$

Figure 2. Scheme of the suction unit.

1: Transmitting optical fibre
2: Receiving optical fibre
3: Optical fibre reflective sensor
4: Back plate of the turbo wheel
5: Si photodiode
6: He-Ne laser (10mW)
7: Oscilloscope LeCroy Waverunner LT322 250MHz
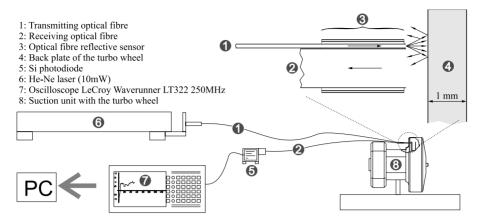8: Suction unit with the turbo wheel

Figure 3. Scheme of the experimental set-up.

Equation (6) shows that the measured signal is distorted in the case of vibration with diametrical nodes and because of the influence of the surface; however, it is not distorted in the case of vibration with circular nodes.

If we use equation (5) together with the equation of vibration with diametrical nodes (1), then the following equation can be derived:

$$N_n(t) = \tfrac{1}{2}[\cos 2\pi(n\nu - \nu_n)t - \cos 2\pi(n\nu + \nu_n)t]. \qquad (7)$$

From equation (7) it is clear that at the rotation frequency ν the natural frequency ν_n of vibration with n diametrical nodes is represented as two frequencies:

$$\hat{\nu}_{n,\min} = |n\nu - \nu_n| \qquad (8)$$

$$\hat{\nu}_{n,\max} = n\nu + \nu_n \qquad (9)$$

where the absolute value is introduced, because the negative frequencies are measured as positive (the cos function is even).

In the case when the frequency ν_n does not depend on the rotation frequency the above two equations (8), (9) are linear functions with respect to ν, and n defines the slope of such a function. Although this is not the case it can help us to characterize the number of diametrical nodes, especially at low rotating frequencies (where $\nu_n \approx$ constant).

3. Experiment

Figure 2 shows the scheme of the suction unit. The measured back plate of the turbo wheel ($\phi120$ mm, diameter of measurement region $\phi110$ mm) is 1 mm thick and constrained to the rotor axis at a diameter of 25 mm. The width of the turbo wheel is 10.5 mm.

3.1. Excitation of vibration

The vibration response under real conditions was of special interest, so the excitation of the vibration was performed with the help of the gyroscopic effect. In reality the suction unit was able to rotate freely round the y axis and an impact force produced a small rotation around it. Because the rotor was rotating around the z axis the gyroscopic response was around the x axis. As a consequence, large deflections were expected at the position of the sensor (figure 2).

3.2. Optical fibre reflective sensor and the inconstant reflection of the surface

The plate displacement was measured using an OFR sensor [9, 10]. These OFR sensors are usually cheap and more convenient when the locating region is restricted. Generally, their measuring range is relatively small (for chosen configuration around 1 mm), and in addition the measured surface needs to be very close to the sensor. Nevertheless, a specially developed OFR sensor proved to be very suitable. The OFR sensor was built from one transmitting glass optical fibre (100 μm core diameter) with NA $= 0.21$ and one receiving glass optical fibre (1000 μm core diameter) with NA $= 0.21$. Both fibres were parallel (spacing $= 550\ \mu$m) with aligned tips and perpendicular to the back plate of the turbo wheel. The distance between the OFR sensor and the turbo-wheel back plate was ≈ 0.5 mm. In agreement with [10], the received optical signal is proportional to the displacement across the whole range of measurement.
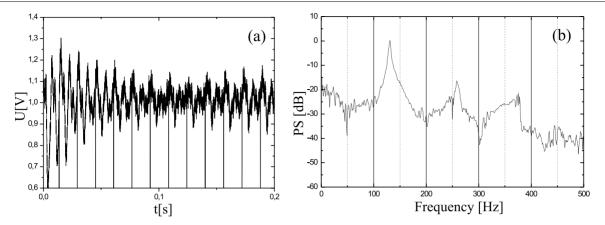
We noticed a variable reflection from the surface. The reason for this is that the plate of the turbo wheel is made of rolled aluminium plate, and so it is oriented in the direction of rolling. This phenomenon can be seen with the unaided eye. Yuan Libo *et al* [12] found some solutions for the automatic intensity compensation, but they are not appropriate for the case of a moving surface.

The additional error is induced by the natural unevenness of the plate. In fact, the impact of the roughness and the natural unevenness (3) of the turbo wheel was partly removed by subtracting the signal which was the case with the relatively slow rotation (and not excited) from the excited signal in the time domain. This could be also done in the frequency domain. However, in the frequency domain the impact of the roughness and natural unevenness shows up as a multiplier of the rotating frequency and as such it can be distinguished from the other frequencies.

The scheme of the experimental set-up is shown in figure 3.

3.3. Results of the experiment

The measurement was made at ten different rotating speeds: 0, 62, 79, 109, 146, 181, 215, 256, 296 and 340 rps (revolutions per second). Each signal was triggered at the moment the impact force was applied and was captured while the transient

Figure 4. The signal of vibration for the case of rotating speed 62 rps ≈ 3720 rpm (*a*). The Fourier transform of (*a*) after the influence of surface roughness and natural unevenness is partly removed (*b*).

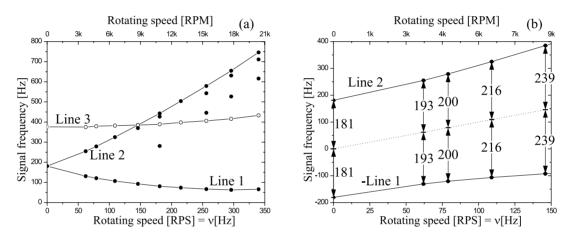**Figure 5.** Energy-carrying frequencies at different rotating speed (*a*). The background of the natural frequency extraction (*b*).
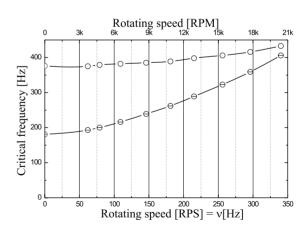
effect was present. Such a signal was then first corrected in terms of the surface roughness and the surface unevenness, and finally transformed into the frequency domain (figure 4). This procedure was repeated for each capture. The maximum measured amplitude of excited vibration was ≈0.25 mm.

The next step was to search for the frequencies carrying a high density of energy. This process is shown in figure 5. Where some points are linked with a curve, the reason is that they are connected with the same vibration mode.

3.4. The extraction of natural frequencies with diametrical nodes

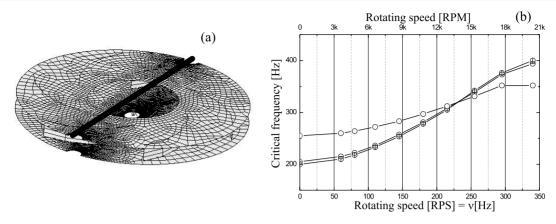Curves 1, 2 and 3 show the changes of the measured frequency with an increased speed of rotation.

At the beginning of curves 1 and 2, their slopes (figure 5) are close to 1 and −1, respectively. This suggests that they are in some way connected with the first natural frequency of the vibration with diametrical nodes ($n = 1$). According to equations (8) and (9), a linear function of rotating frequency, with the slope equal to 1, is drawn (figure 5(*b*)—dotted curve). Additionally, line 1 is drawn as '−line 1'. Because '−line 1' and line 2 are equally distanced from the linear function of the rotating frequency, the suggestion is confirmed. The mentioned distance is the natural frequency of vibration

Figure 6. Natural frequencies (experimental): ⊖ the natural vibration with one diametrical node, ⊙ the natural vibration with no circular nodes.

(equations (8), (9)). The extracted natural frequency is presented in figure 6. Similarly, the natural frequencies of the vibration with *n* diametrical nodes need to be analysed in connection with the linear function of the rotating frequency with slope *n*.

Generally, a dynamic system can have more than one mode with a given number of diametrical nodes. The points near

Figure 7. FEA model with one diametrical node (*a*) and natural frequencies (numerical) (*b*): ⊖ the first natural vibration with one diametrical node; ⊕ the second natural vibration with one diametrical node; ⊙ the natural vibration with no circular nodes.

line 2 (figure 5(*a*)) warn us that the second natural frequency of vibration with one diametrical line is close to the first.

3.5. The extraction of natural frequencies with circular nodes

As derived in the previous section, the signal of natural frequencies with circular nodes does not distort as a consequence of rotation. As 'line 3' seems not to be distorted, we assume that it represents the vibration with circular nodes. Normally, the modes with a higher number of nodes are represented in higher frequencies. As the signal does not include the information about the number of circular nodes (*m*), we assume that this is the lowest natural frequency with no circular nodes (figure 6).

3.6. Discussion

The result of the presented procedure is a rising tendency of the first three natural frequencies in the range from 0 to 24 000 rpm. We suspect that the two natural frequencies of the mode with one diametrical node are very close.

Higher modes of vibration could not be extracted because the vibration amplitudes were too small to be distinguished from the surface unevenness and roughness.

4. Numerical analysis

4.1. The model

This section briefly presents the finite-element analysis (FEA) of the turbo-wheel vibration response. The analysis was only performed for the turbo wheel; other elements of the suction unit were not modelled. The turbo wheel was constrained to the back plate at a diameter of 25 mm. The back and the front plate, as well as the middle vessels, were modelled as two-dimensional shell elements (figure 7(*a*)). The material properties of the aluminium alloy were $E = 70\,000$ MPa, $\rho = 2600$ kg m^{-3} and Poisson ratio = 0.3.

Because of the complexity of a numerical modal analysis of nonlinear systems with nonlinear contact joints, the analysis was modelled so as to be linear. Each vessel was connected to the plate by three pin joints, which is the linear approximation of the real case. Because of back-lash in the joints and because

the deformations were small, the exchange of moment was neglected and thus the use of pin joints was a satisfactory approximation.
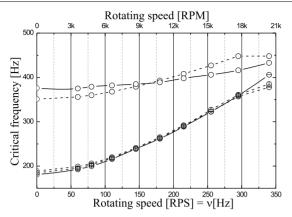
4.2. Results

Figure 7(*a*) shows the first mode with one diametrical node; the second mode with one diametrical node is nearly perpendicular to the first one. Figure 7(*b*) shows the numerically calculated result of a rising tendency of the first three natural frequencies in the range from 0 to 24 000 rpm. As the material properties can differ from those actually used, an analysis with slightly modified properties was also made. In the case when the density was increased from 2600 to 2900 kg m^{-3} ($\approx$12%), the natural frequencies rose by about 5%. The slightly increased diameter of constraint had a negligible influence on the result.

Because a simplified, linear model was used, the results are more qualitative than quantitative.

5. Comparison of results

The numerically obtained natural frequencies of the turbo wheel were made in isolation; other elements of the vacuum-cleaner suction unit were not considered. The numerical results were produced for specific boundary and contact conditions. Because the experiment included the suction unit as a whole, the differences in the results were expected; however, the results were still comparable.

The average difference between numerical results and the experimental in the case of the mode with one diametrical node is 15.8 Hz, and in the case of zero circular lines −96.1 Hz. If the numerical results were shifted by this difference a relatively good agreement was observed (figure 8). An especially good agreement was seen in the case of the diametrical node: in the case of the circular node, the difference is larger. This is partly expected, as the numerical contact conditions (of the vessels)—which produce the error—have a much greater influence on circular nodes than on the radial. The numerical analysis did not consider the flow of air through the suction unit; the flow of air affects the natural frequencies of modes with circular nodes more than those frequencies with the diametrical nodes.

Rotating speed [RPM]

Figure 8. Comparison of the natural frequencies. —— experiment; - - - - shifted numerical analysis. ⊖ the first natural vibration with one diametrical node; ⊕ the second natural vibration with one diametrical node; ⊙ the natural vibration with no circular nodes.

6. Conclusion

The experiment showed some problems with the variable deflection of the laser beam and with the natural unevenness of the turbo-wheel surface, but a bigger problem is the distortion of the signal as the vibrating surface rotates. Therefore, special attention was paid to the interpretation of the measured signal. It became clear that the interpretation of the measured signal is of great importance when the axial displacement of a rotating plane is measured from a stationary point in the surroundings.

The experiment and the numerical analyses were performed in the range from 0 to 20 400 rpm and, after the comparison of the two approaches, we believe that a good agreement was obtained. Therefore, the interpretation of the signal is considered to be correct.

Furthermore, it is assumed that the differences between the two approaches, in the case of the mode with no circular lines, resulted from the simplified numerical model. The numerical analysis was performed for a turbo wheel, separated from the other elements of the suction unit, while the experiment was carried out with the turbo wheel as a part of the suction unit.

As expected, the correlation between the experimental and numerical results was found to be better at lower natural frequencies.

We would like to point out the maximum speed of rotation: 340 rps! Other authors are well below this speed: Ahn *et al* [2] less than 10 rps, Castellini *et al* [4] less than 9 rps and Raman *et al* [3] less than 60 rps. Raman ended at the speed where we begin.

The paper presents work on measuring the actual natural frequencies of a turbo wheel at high rotating speeds and has two major findings: a fibre optic reflective sensor can be used as a displacement sensor for measuring vibrations of rotating structures; and (more importantly) a special method has been developed to extract the frequencies of the vibration from the power spectra.

References

[1] Radcliffe C J and Mote C D Jr 1983 Identification and control of rotating disk vibration *J. Dyn. Syst. Meas. Control* **105** 39–45

[2] Ahn T K and Mote C D Jr 1998 Mode identification of a rotating disk *Exp. Mech.* **38** 250–4

[3] Raman A and Mote C D Jr 2001 Experimental studies on the non-linear oscillations of imperfect circular disks spinning near critical speed *Int. J. Non-Linear Mech.* **36** 291–305

[4] Castellini P and Santolini C 1998 Vibration measurements on blades of a naval propeller rotating in water with tracking laser vibrometer *Measurement* **24** 43–54

[5] Bucher I, Robb D A, Schmiechen P and Ewins D J 1994 A laser-based measurement system for measuring the vibration on rotating discs *1st Int. Conf. on Vibration Measurements by Laser Techniques* pp 398–408

[6] Zielinski M and Ziller G 2000 Noncontact vibration measurements on compressor rotor blades *Meas. Sci. Technol.* **11** 847–56

[7] Heath S and Imregun M 1997 A review of analysis techniques for blade tip-timing measurements *Int. Gas Turbine and Aeroengine Congr. Exhibition (Orlando, FL, 1997)* ASME 97-GT-213

[8] Dhadwal H S, Mehmud A and Khan R 1996 Integrated fiber optic light probe: measurement of static deflections in rotating turbomachinery *Rev. Sci. Instrum.* **67** 546–52

[9] Suhadolnik A, Babnik A and Možina J 1995 Optical fiber reflection refractometer *Sensors Actuators* B **29** 428–32

[10] Cook R O and Hamm C W 1979 Fiber optic lever displacement transducer *Appl. Opt.* **18**

[11] Kadambi J R, Reinhardt A K and Quinn R D 1994 Laser vibrometry measurements of rotating blade vibrations *8th Congr. Exposition of Gas Turbine Institute* pp 453–61

[12] Libo Y and Anping Q 1991 Fiber-optic diaphragm pressure sensor with automatic intensity compensation *Sensors Actuators* A **28** 29–33